Accepted Manuscript

Comparing coronary stent material performance on a common geometric platform through simulated bench-testing

J.A. Grogan, S.B. Leen, P.E. McHugh

PII: S1751-6161(12)00064-1
DOI: 10.1016/j.jmbbm.2012.02.013
Reference: JMBBM 538

To appear in: *Journal of the Mechanical Behavior of Biomedical Materials*

Received date: 19 December 2011
Revised date: 14 February 2012
Accepted date: 19 February 2012

Please cite this article as: Grogan, J.A., Leen, S.B., McHugh, P.E., Comparing coronary stent material performance on a common geometric platform through simulated bench-testing. *Journal of the Mechanical Behavior of Biomedical Materials* (2012), doi:10.1016/j.jmbbm.2012.02.013

Comparing coronary stent material performance on a common geometric platform through simulated bench-testing.

J.A. Grogan, S.B. Leen, P.E. McHugh

Biomechanics Research Centre (BMEC), Mechanical and Biomedical Engineering, College of Engineering and Informatics, National University of Ireland, Galway, Ireland.

E-mail: j.grogan1@nuigalway.ie (J. A. Grogan).

Abstract

Absorbable metallic stents (AMS) are a newly emerging cardiovascular technology which has the potential to eliminate long-term patient health risks associated with conventional, permanent stents. AMS developed to date have consisted of magnesium alloys or iron, materials with inferior mechanical properties to those used in permanent stents, such as stainless steel and cobalt chromium alloys. However, for AMS to be feasible for widespread clinical use it is important that their performance is comparable to modern, permanent stents. To date, the performance of magnesium, iron and permanent stent materials have not been compared on a common stent platform for a range of stent performance metrics, such as flexibility, radial strength and recoil. In this study this comparison is made through simulated bench-testing, based on finite element modelling. The significance of this study is that it allows potential limitations in current AMS performance to be identified, which will aid in focusing future AMS design. This study also allows the identification of limitations in current AMS materials, thereby informing the on-going development of candidate biodegradable alloys. The results indicate that the AMS studied here can match the recoil characteristics and radial strength of modern, permanent stents; however, to achieve this, larger strut dimensions are required. It is also predicted that the AMS studied are inferior to permanent stents in terms of maximum absolute curvature and longitudinal stiffness.

Keywords: finite element analysis, biodegradable iron, biodegradable magnesium, absorbable metallic stents

Introduction

Coronary stents are small, cylindrical scaffolds used in the treatment of atherosclerosis. The primary role of the stent is to prevent elastic arterial recoil following vessel dilation with an angioplasty balloon (Serruys et al., 1994). Typically coronary stents have been considered to be permanent implants, consisting of high-strength, corrosion-resistant alloys such as stainless steel (316L) and cobalt chromium L605 (CoCr). However, stents that are gradually absorbed in the body are now attracting much interest (Peuster et al., 2006). This is due to the possibility of eliminating the risk of late-stent thrombosis, associated with the long-term presence of the stent, and also reducing the need for prolonged anti-platelet therapy (Waksman, 2007).

Absorbable metallic stents (AMS) have shown promise in preliminary clinical trials (Erbel et al., 2007), however in order for AMS to be accepted into widespread clinical use it must be proven that their performance can at least match that of modern, permanent stents. As shown in Fig. 1 and Table 1, the mechanical properties of typical bioabsorbable metals developed to date are generally inferior to those of permanent stent materials, such as 316L and CoCr. This makes the design of AMS more challenging than that of permanent stents (Deng et al., 2011) and leads to a question on the ability of current AMS to match permanent stent performance in terms of stent radial strength, recoil and flexibility.

Simulated bench-testing based on finite element (FE) modelling is commonly used in contrasting the performance of different permanent stents (Etave et al., 2001; Migliavacca et al., 2002; Mortier et al., 2011). This study employs a similar approach in investigating the ability of AMS to match the performance of permanent stents over metrics such as radial strength, recoil and flexibility. To date, a small number of FE studies have investigated the performance of magnesium alloy stents (Wu et al., 2010; Gastaldi et al., 2011; Grogan et al., 2011) with predicted device stresses, strains and recoil reported. However, to the authors' knowledge, this is the first study in which the performances of magnesium alloy, iron and permanent stents have been directly contrasted on a common stent geometry over a range of performance metrics, such as radial strength and flexibility. Also, to the authors' knowledge, this is the first computational study in which stent resistance to longitudinal compression is compared over a range of materials, with the ability of coronary stents to resist longitudinal compression recently emerging as a concern in device design (Prabhu et al., 2011). The significance of the study is that it

facilitates the identification of current limitations in AMS performance and also allows recommendations to be made on how current biodegradable metals can be improved to allow AMS to more closely match the performance of permanent stents.

The adoption of a common geometric platform across materials in this study allows a direct comparison of a material's performance in a stent application with that of established stent materials. However, given that AMS designs used in *in-vivo* studies to date (Erbel et al., 2007; Peuster et al., 2001) differ somewhat from the common geometry used here, and that some may be designed based on the mechanical properties of a specific alloy, it is useful to also consider the performance of designs representative of those tested *in-vivo*, alongside that of the common geometry.

As such, the specific goals of this study are: 1) to compare AMS and permanent stent performance using: i) a common stent geometry and ii) representative stent geometries, through FE modelling, 2) to identify current design challenges facing AMS development, based on model predictions, and 3) to make recommendations toward the on-going development of candidate biodegradable metals for improved AMS performance.

Methods

Stent bench-testing was simulated using the Abaqus/Explicit commercial FE code (DS SIMULIA, RI, USA), assuming finite deformation kinematics. The performances of candidate biodegradable alloys were assessed on a generic stent geometry (geometry A in Fig. 2), allowing a direct comparison of material performance across a common geometric platform, and also on geometries representative of those used in previous *in-vivo* experiments on magnesium alloy stents (Erbel et al., 2007) and iron stents (Peuster et al., 2001). Information on the studied geometries is given in Fig. 2 and Table 2.

Six stent materials were studied in each bench-test. Conventional stent materials stainless steel 316L and cobalt chromium L605 were studied on generic geometry A, described in Table 2, with L605 also studied on geometry A1, which has the same underlying design as geometry A, but strut dimensions similar to those of many modern 'thin-strut' stents. Magnesium alloys AZ31 and WE43, which is the alloy used in the clinical trials of Erbel et al., (2007), were studied using generic geometry A and also geometry B, which is representative of the 'Magic' stent geometry

used in the trial of Erbel et al., (2007). Two forms (denoted T1 and T2) of annealed pure iron, which has been used in the *in-vivo* studies of Peuster et al., (2001), were considered in this study, with different mechanical properties arising from different annealing heat treatments. The performance of the pure iron was assessed on the generic geometry A and geometry C, which is representative of the 'PUVA' stent used in the study of Peuster et al., (2001).

Stress-strain data for each material was taken from the literature, as detailed in Table 1 and Fig. 1. Each material was modelled using a rate-independent elastic-plastic material description, with elasticity assumed linear in terms of finite deformation quantities, in particular Cauchy stress and Lagrangian strain, (DS SIMULIA, 2010), and plasticity described using J_2 flow theory with non-linear isotropic hardening. The finite element meshes used to discretise each geometry, shown in Fig. 2, were chosen based on the results of preliminary solution mesh dependence studies. In order to ensure a negligible influence of inertial effects when using the Abaqus/Explicit code, the ratio of kinetic energy to internal energy of less than 0.05 was maintained in all simulations.

Four bench-tests were simulated for each material and geometry, as detailed in Fig. 3. In the first test, stent deployment and recoil were simulated through the expansion to 3.0 mm and subsequent contraction of a rigid cylindrical shell, as shown in Fig. 3. This approach has been used in a number of previous studies (Gervaso et al., 2008; Wu et al., 2011) and has been shown by De Beule et al. (2008) to give an accurate prediction of the final, deployed stent geometry for unconfined, straight stent expansions relative to that achieved in more computationally expensive wrapped balloon simulations, such as those of Mortier et al. (2010) and Grogan et al. (2011). For this study the extra control over final stent diameter afforded by cylinder deployment for each material and geometry also proved advantageous.

The quantities of interest in the first test are peak von-Mises stresses (σ_e), max principal logarithmic strains (ε_{mp}) and stent recoil. Von-Mises stresses are chosen as a simple measure of maximum device stress in this case, given the ductile nature and large plastic deformations of the metals considered in this study, with alternative measures such as maximum principal stresses also giving similar overall trends in terms of device performance. In order to facilitate a comparison of peak stresses and strains across each material, an appropriate comparative indicator is required. For this study a straight-forward approach was chosen in comparing materials, through the definition of respective stress and strain based factors of safety, η_σ and η_ε.

In determining each factor of safety, predicted peak stresses and strains in the stent were compared with estimates of true stress and strain at the point of ultimate tensile stress (UTS) in each material's engineering stress-strain curve. A conventional conversion of engineering to true stress and logarithmic strain measures (Callister et al., 2007) was used, based on UTS (σ_{UTS}) and engineering strain at UTS (ε_{UTS}) data for each material, given in Table 1. This gave the following factor of safety definitions:

$$\eta_\sigma = \frac{(1+\varepsilon_{UTS})\sigma_{UTS}}{\sigma_e} \tag{1}$$

$$\eta_\varepsilon = \frac{\log_e(1+\varepsilon_{UTS})}{\varepsilon_{mp}} \tag{2}$$

In quantifying stent recoil a conventional approach was taken (Migliavacca et al., 2002), with recoil given by:

$$\text{Recoil} = \frac{D_1 - D_2}{D_1} \times 100\% \tag{3}$$

where D_1 is the stent internal diameter at max expansion and D_2 is the stent internal diameter following rigid cylinder contraction.

To assess the ability of the two ring geometries used in this study to capture the η_σ and η_ε values and overall recoil behaviour of each material in a longer stent, a preliminary deployment simulation of a four ring generic stent, half of which was modelled due to longitudinal symmetry, with a wrapped balloon was performed. Results were compared to those from a cylinder deployment of a two ring generic stent. It was observed that the final stent configurations were very similar, as shown in Fig. 4, with only a 1.1% higher peak Von Mises stress and a 0.09% lower stent recoil magnitude predicted for the wrapped balloon simulation. Such differences result in minor over-estimations in η_σ (1.1%) and recoil (0.09%) values for the cylinder deployment method, but these over-estimations are small relative to the range of values each metric takes over the different materials tested in this study.

In the second test, stent radial strengths were predicted for each material. Radial compression of each stent was simulated by introducing a thin elastic sheath over the deployed stent, as shown in Fig. 3. An inward pressure was applied to the outer surface of the sheath and transferred to the

stent by contact. The sheath was sufficiently compliant as to not support a significant inward pressure by itself (Young's modulus, E = 0.1 GPa; Poisson's Ratio, ν = 0.4) and was constrained to only deform radially with respect to the stent's longitudinal axis. The collapse behaviour of the stent was quantified through the determination of a pressure-diameter curve, with the stent outer diameter (D) determined for a given applied pressure. Due to there being no obvious point of global collapse, the pressure for 10% diameter loss, relative to the unloaded stent outer diameter, D_0, was taken as a measure of stent radial strength in this study. This diameter loss corresponds to a clear deviation from linear behaviour in the pressure-diameter curve for all stents.

The third test predicted stent resistance to longitudinal compression. All nodes on each end of the deployed stent geometry were fixed to control nodes by means of multi-point constraints, as shown in Fig. 3. The right control node was then moved toward the left control node, which was fixed in all directions, under displacement control. The resulting reaction force on the right node was taken as a measure of resistance to a given amount of stent longitudinal compression, consistent with the measure used in the experiments of Prabhu et al. (2011).

The final test predicted the stent's flexibility, in terms of both elastic and plastic deformations. The approach taken was similar to that commonly used in FE stent flexibility studies (Petrini et al., 2004; Wu et al., 2007; Pant et al., 2011) and allowed a direct comparison with previous experimental studies (Mori and Saito, 2005). Similar to the previous bench-tests, only two circumferential rings of the stent were modelled for stents A and C and three for stent B. This simplification, which allows improved computational efficiency, can give a good approximation of the flexibility of a longer stent with the same repeating unit (Petrini et al., 2004). In the present study, each end of the stent was fixed in all directions to two control nodes via multi-point-constraints, the right control node was then rotated about the left control node through an angle θ, as shown in Fig. 3. In an approach similar to that of the previously mentioned FE studies, stent flexibility was determined in terms of the resulting moment-curvature curve, with the moment given by the reaction moment on the right-control node and the curvature (κ) given by:

$$\kappa = \frac{\theta}{L_U} \tag{4}$$

where L_U is the length of the stent unit. Stent flexibility was quantified as the inverse slope of the linear (elastic) portion of the moment-curvature curve, allowing a comparison of model predictions with the experiments of Mori and Saito, (2005).

Results

Figs. 5(a) and (b) show the respective η_σ and η_ε values for each material and geometry. It is predicted that all studied magnesium alloy stents have significantly lower η_σ and η_ε values than the CoCr and 316L stents at maximum expansion. The iron stents are predicted to generally have η_σ and η_ε values closer to those of the permanent stents, with the iron T2 generic stent having comparable values to the permanent stents. Predicted recoil for the 316L stent (3.9%), as shown in Fig. 5(c), is in good agreement with that measured experimentally for the Cypher stent (3.4%) (Menown et al., 2010), while the higher recoil predicted in the thin CoCr stent (6.7%) is consistent with experimental measurements of higher recoils in modern thin-strut stents, for example the Multilink Vision stent (5.9%) (Lanzer, 2007). The relatively high recoils predicted in the magnesium alloy stents (4.7% - 8.6%) are in agreement with reported stent recoil of under 8% for the Biotronik Magic magnesium alloy stent (Erbel et al., 2007), while the relatively low recoils predicted for the iron stents (0.9% - 1.6%) are in agreement with the experimental studies of Peuster et al. (2001), who reported a recoil of 2.2%.

Figs. 6 (a) and (b) show the predicted pressure-diameter curves for selected stents and the pressure required for 10% diameter loss for all stents. Agrawal et al. (1992) have suggested a minimum collapse pressure of 0.04 MPa for coronary stents. Modern CoCr stents have typical collapse pressures of just over 0.1 MPa (Schmidt et al., 2009), with some older 316L stents having collapse pressures as high as 0.21 MPa (Venkatraman, 2003). This range shows good agreement with the stent radial strength predictions in this study of 0.08 - 0.15 MPa for 10 and 50% diameter loss in the 80 m CoCr stent and 0.16 - 0.25 MPa for the 316L stent. The lower radial strengths of the magnesium alloy stents predicted in this study (0.06 - 0.14 MPa for 10 and 50% diameter loss) are in good agreement with the reported collapse pressure of 0.08 MPa for the Biotronik Magic magnesium alloy stent (Erbel et al., 2007).

As shown in Fig. 7(a), it is predicted that the AMS have greater flexibility than the permanent stents, including the 80 m CoCr stent. However, as shown in Fig. 7 (b), the curvatures at which the AMS reach a η_ε value of 1.0 are somewhat lower than those of the permanent stents. Moment-curvature predictions for the 316L stent in this study show good qualitative and quantitative agreement with those of Pant et al. (2011), who simulated flexure in a similar stent geometry. Also, considering only the linear portion of the moment-curvature behaviour, predicted flexibility for the 316L stent (0.0062 $N^{-1}mm^{-2}$) falls within the range of 316L stent flexibilities experimentally investigated by Mori and Saito (2005) of 0.0053 – 0.024 $N^{-1}mm^{-2}$.

Figs. 8 (a) and (b) shows the predicted resistance of selected stents to an applied longitudinal compression and the reaction force required for 10% compression of all stents. The predicted force of 2.8 N required for a 6.5% compression of the 316L stent differs from the force of 0.5 N for the same compression of the Cypher stent observed experimentally in Prabhu et al. (2011). This difference is possibly due to the different connecting section geometries of the stent studied here and the Cypher stent, with stent geometry contributing significantly to device compressive resistance (Prabhu et al., 2011). Insufficient resistance to stent longitudinal compression is undesirable as it increases the risk of stent-artery malapposition if the stent comes into contact with the delivery system following deployment. In this study, it is predicted that the AMS have a significantly lower resistance to longitudinal compression than the permanent stents. It is also predicted that reducing the strut dimensions from 120 to 80 m in the CoCr stent resulted in a significant reduction in resistance.

Discussion

The very low η_ε values (< 1.1) predicted in this study for both magnesium alloys and the generic and representative magnesium stent designs, relative to those of the modern CoCr and 316L stents (> 2.6), suggest that considerable effort is required in terms of both device and alloy design to ensure a comparable fracture risk with modern, permanent stents. Addressing such a risk is of particular importance considering the nature of the relatively undemanding tests considered here, where additional deformations due to arterial curvature or irregular lumen geometry were not considered. Alloy specific device design, through geometric parameter studies and shape optimization based on finite element analysis seem necessary in the further development of such stents, with early applications of such an approach showing promise (Wu et

al., 2010). Despite this promise, given the large gap in predicted η_ε values between the magnesium and permanent stents, it is likely that improved alloy ductility relative to the AZ31 and WE43 alloys studied here is necessary before comparable performance in this regard can be achieved. In terms of the pure iron, it is predicted that η_ε values more comparable with permanent stents are achievable (up to 2.1), with it likely that similar performance is possible for this metric through careful stent design.

The low maximum curvatures predicted for both magnesium stent designs and alloys (< 0.15 mm^{-1}) relative to the modern, permanent stents (>0.75 mm^{-1}) also suggest that significant effort is also required in terms of improved stent design to ensure strains in stent connecting links are minimized and improved alloy design in terms of increased ductility. This is particularly important considering typical natural arterial curvatures of up to 0.066 mm^{-1} in 90% of the population (Liao et al., 2004), with variations of 0.025 – 0.18 mm^{-1} reported during the cardiac cycle (Gross et al., 1998). In the case of iron stents, maximum curvatures of up to 0.33 mm^{-1} were predicted, which gives an improved performance over the magnesium stents, but may still require careful design of stent connecting links to allow comparable performance with permanent stents.

In terms of recoil, a reasonable performance is predicted for the magnesium stents, (4.7 – 8.6%) relative to the thin CoCr stent (6.7%), however it is important to note the larger strut cross-sections of the simulated magnesium stents (0.0144 – 0.0154 mm^2) relative to the CoCr stent (0.006 mm^2). Interestingly, the recoil performance of the iron stents (1.6%) is predicted to be significantly better than even the permanent stents. In terms of radial strength, similar performance is noted for the magnesium (0.06 – 0.073 MPa), iron (0.06 – 0.09 MPa) and thin CoCr stents (0.082 MPa), again noting the larger cross-sectional areas of the biodegradable stents. These recoil and radial strength results suggest that the studied materials have sufficient yield strengths (138 - 216 MPa) and UTS (245 - 298 MPa) to achieve comparable scaffolding ability with permanent stents, albeit through the use of designs with larger strut dimensions.

It is noted in these comparisons that the iron stents show good potential in terms of achieving comparable performance with permanent stents across most metrics. However, in the future development of iron stents it is of interest to reduce strut dimensions insofar as possible, in order to compensate for the relatively low rate of iron degradation in-vivo (Hermawan et al., 2010). In

allowing for such a reduction it appears, based on model predictions, that device radial strength is the limiting performance metric. As such, the development of higher strength (yield and UTS) iron alloys would be highly beneficial in the future development of iron stents, with newly developed alloys such as Fe35Mn (Hermawan et al., 2010) showing much promise in this regard. Such reductions in device dimensions would also prove beneficial in terms of improvements in device fracture risk and maximum curvature.

Limitations

Modelling approaches used in this study are either in line with the published literature, or, when established modelling methods aren't available, predictions are compared directly to results of *in-vitro* experiments. However, some limitations to the study must be acknowledged.

Currently a wide range of magnesium and iron alloys are under consideration for stent application (Moravej, 2011), only four of which were considered in this study. While the authors believe the chosen magnesium alloys are representative of the general behaviour of magnesium alloys in development, it would prove useful in a further study to repeat the simulated tests for an extended range of candidate alloys, using results presented here as an initial benchmark. In the case of iron, it would be of interest to compare the performance of pure iron with that of newly developed iron alloys such as Fe35Mn.

Stent struts are small metallic components, with typically only a few metallic grains through their thickness. As such, continuum plasticity theory and material stress-strain data based on tensile testing of large-size samples, as used in this study, may not fully capture experimentally observed ductility size-effects in coronary stent struts (Murphy et al., 2003). Improved predictive capabilities could be afforded through the use of micro-scale modelling based on crystal plasticity theory (Harewood and McHugh, 2007). Such a study would be particularly significant in the case of annealed pure iron, which can have large grain sizes (20 m for iron-T1 as per Carson et al., 1968 and 35 m for iron-T2 as per Islam et al., 2011) relative to those typical of 316L (10 m as per Murphy et al., 2003).

Only short-term stent performance is considered in this study. Over time magnesium and iron stents will corrode in the body and loose scaffolding ability. The design of these devices and candidate alloys may be further restricted than indicated in this study by the need to ensure

suitable device corrosion behaviour. Such restrictions can be investigated through the application of FE based corrosion models, such as that of Grogan et al. (2011). Further to this, the risk of device failure in fatigue should be studied, incorporating the roles device micro-mechanics and corrosion on fatigue life.

Conclusions

This study presents a computational investigation into the role of material choice on coronary stent performance for magnesium alloy, iron, steel and cobalt chromium stents, based on generic and alloy specific geometric platforms. Stent performance was assessed through simulated bench-testing, using modelling techniques that have either been well established in the literature or have predictions that can be readily compared with the results of *in-vitro* experiments. The following are some key conclusions from this work:

- A significantly higher device fracture risk was predicted in deployment for the magnesium stents than the permanent or iron stents.
- Respective maximum allowable device curvatures in the magnesium and iron stents were predicted to be less than 20% and 50% of those of the permanent stents.
- Resistances to longitudinal compression in the magnesium and iron stents were predicted to be less than 50% of those of the permanent stents.
- The struts of the magnesium and iron stents studied here require cross-sectional areas 2.4 and 1.5 times greater, respectively, than the modern CoCr stent for comparable performance in terms of radial strength and recoil.
- In terms of magnesium alloy stent development, the results presented indicate that alloy ductility needs to be increased by a factor of up to 3 for comparable performance with modern stents, vis-à-vis predicted fracture risk, with it strongly recommended that the ductility of alloys proposed for AMS application at least matches that of the AZ31 and WE43 alloys studied here.
- For iron stents, future research should focus on the development of higher strength iron alloys, allowing smaller strut dimensions that are more accommodating of the low *in-*

311 *vivo* corrosion rates of iron and that are comparable to those of modern, permanent
312 stents.

313 ## Acknowledgements

314 The authors acknowledge the SFI funded Irish Centre for High End Computing (ICHEC) for the
315 provision of computational resources and support and project funding by an IRCSET fellowship
316 (J. Grogan) under the EMBARK initiative.

317 ## References

318 Agrawal, C.M., Haas, K.F., Leopold, D.A., Clark, H.G., 1992. Evaluation of poly(L-lactic acid)
319 as a material for intravascular polymeric stents. Biomaterials. 13, 176-182.

320 Callister, W.D., Rethwisch, D.G., 2007, Fundamentals of Materials Science and Engineering: An
321 Integrated Approach, third ed., John Wiley & Sons, Inc., Honoken, NJ, USA.

322 Carson, J.M., Hawn, J.M., 1968. Some Properties of Iron, Copper, and Selected Aluminium
323 Alloys including True Stress-True Strain at Reduced Temperatures. Air Force Materials
324 Laboratory, Technical Report Number 68-251, University of Dayton Research Institute,
325 Dayton, OH, USA.

326 De Beule, M., Mortier, P., Carlier, G., Verhegghe, B., Van Impe, R., Verdonck, P., 2008.
327 Realistic finite element-based stent design: The impact of balloon folding. J. Biomech.,
328 41, 383-389.

329 Deng, C.Z, Radhakrishnan, R., Larsen, S.R., Boismer, D.A., Stinson, J.S., Hotchkiss, A.K. ,
330 Petersen, E.M., et al., 2011, Magnesium Alloys For Bioabsorbable Stents: A Feasibility
331 Assessment, in: Sillekens, W.H., Agnew, S.R., Neelameggham, N.R., Mathaudhu, S.N.,
332 (Eds.), Magnesium Technology 2011, John Wiley & Sons, Inc., Honoken, NJ, USA, pp.
333 413-418.

334 DS SIMULIA, 2010. Abaqus 6.10 Theory Manual, DS SIMULIA Corp., Providence, RI, USA.

335 Erbel, R., Di Mario, C., Bartunek, J., Bonnier, J., de Bruyne, B., Eberli, F.R., Erne, P. et al.,
336 2007. Temporary scaffolding of coronary arteries with bioabsorbable magnesium stents:
337 a prospective, non-randomised multicentre trial. Lancet. 369, 1869-1875.

338 Etave, F., Finet, G., Boivin, M., Boyer, J.C., Rioufol, G., Thollet, G., 2001. Mechanical
339 properties of coronary stents determined by using finite element analysis. J.Biomech. 34,
340 1065-1075.

341 Gastaldi, D., Sassi, V., Petrini, L., Vedani, M., Trasatti, S., Migliavacca. F., 2011. Continuum
342 damage model for bioresorbable magnesium alloy devices — Application to coronary
343 stents. J. Mech. Behav. Biomed. Mater., 4, 352-365.

344 Grogan, J.A., O'Brien, B.J., Leen, S.B., McHugh, P.E., 2011. A corrosion model for
345 bioabsorbable metallic stents. Acta. Biomat. 7, 3523-3533.

346 Gross M.F. and Friedman, M.H., 1998. Dynamics of coronary artery curvature obtained from
347 biplane cineangiograms. J Biomech., 31, 479-484,

348 Gu, X.N., Zhou, W.R., Zheng, Y.F., Cheng, Y., Wei ,S.C., Zhong, S.P., Xi, T.F., et al., 2010.
349 Corrosion fatigue behaviors of two biomedical Mg alloys - AZ91D and WE43 - In
350 simulated body fluid. Acta Biomat. 6, 4605-4613.

351 Harewood, F.J., McHugh, P.E., 2007. Modeling of Size Dependent Failure in Cardiovascular
352 Stent Struts under Tension and Bending. Ann. Biomed. Eng., 35,1539-1553.

353 Hermawan, H., Dubé, D. & Mantovani, D., 2010. Developments in metallic biodegradable
354 stents. Acta Biomaterialia, 6(5), pp.1693-1697.

355 Islam, M.A., Sato, N.,Tomota, Y., 2011. Tensile and plane bending fatigue properties of pure
356 iron and iron-phosphorus alloys at room temperature in the air. Trans. Indian Inst. Metal.,
357 64, 315-320.

358 Lanzer, P., 2007. Mastering endovascular techniques: a guide to excellence. Lippincott Williams
359 & Wilkins, Philadelphia, PA, USA.

360 Liao, R., Green, N.E., Chen, S.Y.J., Messenger, J.C., Hansgen, A.R., Groves, B.M., Carroll, J.D.,
361 2004, Three-dimensional analysis of in vivo coronary stent--coronary artery interactions.
362 Int. J. Cardiovasc. Imaging, 20, 305-313.

363 Menown, I.B.A., Noad, R., Garcia, E.J., Ian Meredith, I., 2010. The platinum chromium element
364 stent platform: from alloy, to design, to clinical practice. Advances in Therapy 27, 129-
365 141.

366 Migliavacca, F., Petrini, L., Colombo, M., Auricchio, F., Pietrabissa, R., 2002. Mechanical
367 behavior of coronary stents investigated through the finite element method. J. Biomech.
368 35, 803-811.

369 Moravej, M., Mantovani, D., 2011. Biodegradable Metals for Cardiovascular Stent Application:
370 Interests and New Opportunities. Int. J. Mol. Sci., 12, 4250-4270.

371 Mori, K., Saito, T., 2005. "Effects of Stent Structure on Stent Flexibility Measurements." Ann.
372 Biomed. Eng. 33, 733-742.

373 Mortier, P., De Beule, M., Segers,P., Verdonck, P., Verhegghe.B., 2011. Virtual bench testing of
374 new generation coronary stents. EuroIntervention. 7, 369-376.

375 Mortier, P., Holzapfel, G.A., De Beule, M., Denis Van Loo, M., Taeymans, Y., Segers, P.,
376 Verdonck, P. et al., 2010. A novel simulation strategy for stent insertion and deployment
377 in curved coronary bifurcations: comparison of three drug-eluting stents. Ann. Biomed.
378 Eng. 38, 88-99.

Muller, H., 2009, Development of metallic bioabsorbable intravascular implants. In: Chakfé, B., and Durand, B. (Eds), New Technologies in Vascular Biomaterials. Connecting Biomaterials to Arterial Structures, Strasbourg, Europrot, pp. 23–32.

Murphy, B.P., Savage, P., McHugh, P.E., Quinn. D.F., 2003. The stress-strain behavior of coronary stent struts is size dependent. Ann. Biomed. Eng.31, 686-691.

Pant, S., Bressloff, N.W., Limbert. G., 2011. Geometry parameterization and multidisciplinary constrained optimization of coronary stents. Biomech. Model. Mechanobiol. (In Press) doi:10.1007/s10237-011-0293-3.

Petrini, L., Migliavacca, F., Auricchio, F., Dubini, G., 2004. Numerical investigation of the intravascular coronary stent flexibility. J. Biomech., 37, 495-501.

Peuster, M., Wohlsein, P., Brugmann, M., Ehlerding, M., Seidler, K., Fink, C., Brauer, H., et al., 2001. A novel approach to temporary stenting: degraPONCIdable cardiovascular stents produced from corrodible metal—results 6-18 months after implantation into New Zealand white rabbits. Heart. 86, 563-569.

Peuster, M., Beerbaum,P., Bach, F.W., Hansjoerg Hauser. H., 2006. Are resorbable implants about to become a reality?. Card. Young. 16, 107-116.

Poncin, P., Proft., J.,2004, Stent Tubing: Understanding the Desried Attributes, in: Shrivastava, S., (Ed.), Medical device materials: proceedings from the Materials & Processes for Medical Devices Conference 2003, 8-10 September 2003, Anaheim, California. ASM International, OH, USA.

Prabhu, S., Schikorr, T., Mahmoud, T., Jacobs, J., Potgieter, A., Simonton, C., 2011. Engineering assessment of the longitudinal compression behaviour of contemporary coronary stents. EuroIntervention. (In Press), http://www.ncbi.nlm.nih.gov/pubmed/22057097.

Schmidt, W., Behrens, P., Schmitz, K.P., 2009, Biomechanical Aspects of Potential Stent Malapposition at Coronary Stent Implantation, in: Dössel, O., Schlegel, W.C., (Eds.), World Congress on Medical Physics and Biomedical Engineering: Surgery, Minimal Invasive Interventions, Endoscopy and Image Guided Therapy, Springer, pp. 136-139.

Serruys, P.W., de Jaegere, P., Kiemeneij, F., Macaya, C., Rutsch, W., Heyndrickx, G., H Emanuelsson, H., et al., 1994. A comparison of balloon-expandable-stent implantation with balloon angioplasty in patients with coronary artery disease. Benestent Study Group. New Eng. J. Med. 331, 489-495.

Tsunoda, T., Nakamura, M., Wada, M., Ito, N. Kitagawa, Y., Shiba, M. Yajima, S.,et al., 2004. Chronic stent recoil plays an important role in restenosis of the right coronary ostium. Cor. Art. Dis. 15, 39-44.

Venkatraman, S., Poh, T.L., Vinalia, T., Mak, H.K., Boey.F, 2003. Collapse pressures of biodegradable stents. Biomaterials. 24, 2105-2111.

Waksman, R., 2007. Promise and challenges of bioabsorbable stents. Catheter. Cardio. Int. 70, 407-414.

Werkhoven, R.J., Sillekens, W.H. & van Lieshout, J.B.J.., Processing Aspects of Magnesium Alloy Stent Tube. , pp.419-424.

Wu, W., Petrini, L., Gastaldi, D., Villa, T., Vedani, M., Lesma, E., Previtali, B., Migliavacca. F., 2010. Finite element shape optimization for biodegradable magnesium alloy stents. Ann. Biomed. Eng. 38, 2829-2840.

Wu, W., Yang, D.Z., Qi, M., Wang. W.Q., 2007. An FEA method to study flexibility of expanded coronary stents. J. Mat. Proc.Tech. 184, 447-450.

Wu, W., Gastaldi, D., Yang, K., Tan, L., Petrini, L., Migliavacca, F., 2011. Finite element analyses for design evaluation of biodegradable magnesium alloy stents in arterial vessels. Mat. Sci.and Eng.:B, 176, 1733-1740.

444 Tables

Material	**Young's** Modulus (GPa)	Yield Strength (MPa)	Ultimate Tensile Strength (MPa)	Strain at UTS (%)	Source
Stainless Steel - 316L	190	380	750	51	(Murphy *et al.*, 2003)
Cobalt Chromium - L605	243	629	1147	46	(Poncin *et al.*, 2003)
Magnesium Alloy - WE43	45*	216	298	18	(Gu *et al.*, 2010)
Magnesium Alloy - AZ31	44	138	245	17	(Grogan *et al.*, 2011)
Pure Iron - Treatment 1	211	138	282	25	(Carson *et al.*, 1968)
Pure Iron - Treatment 2	211	170	270	36	(Islam *et al.*, 2011)

445 * Source: Muller et al., 2009

446 Table 1. Mechanical properties for each material considered in this study, including the sources
447 of the stress-strain data shown in Fig. 1.

448

Stent	Similar to:	Source:	Strut Width (μm)	Strut Thickness (μm)	Length (mm)	FE Mesh
A	Generic	(Pant *et al.*, 2011)	120	120	3.30	66,000
A1	Generic	(Pant *et al.*, 2011)	80	80	3.26	108,000
B	Magic Stent	SEM Images (Erbel *et al.*, 2007)	80	140	3.18	76,000
C	PUVA Stent	Microscope Images (Peuster *et al.*, 2001)	80	120	2.70	61,500

449

450 Table 2. Stent geometries used in this study. Each geometry has a pre-deployment outer
451 diameter, D, of 1.5 mm and is meshed using reduced integration 3D linear brick elements
452 (C3D8R). The number of elements used in each geometry is shown in the column 'FE Mesh'.
453 'Width' refers to the circumferential strut dimension and 'thickness' refers to the radial strut
454 dimension.

455

456

457

458

459 Figures

460 Figure. 1. Engineering stress-strain curves for each material modelled in this study. The source
461 of each stress-strain curve is shown in Table 1.

462 Figure. 2. Stent geometries used in this study and corresponding finite element meshes.
463 Geometry details are given in Table 2.

464 Figure. 3. Schematic representation of the test cases simulated.

465 Figure. 4. A comparison of von-Mises stresses in the magnesium alloy stent following expansion
466 by balloon deployment and a rigid cylinder. Very similar stress distributions and overall stent
467 deformed geometry were predicted for both cases.

468 Figure. 5. Predicted factors of safety, (a) η_σ and (b) η_ε, for each stent material and geometry. (c)
469 Predicted elastic recoil for each stent.

470 Figure. 6. (a) Predicted loss in stent outer diameter (D) relative to its unloaded diameter (D_0) due
471 to an external applied pressure for selected stents. (b) The applied pressure required to give a
472 10% stent diameter reduction for all materials and stents.

473 Figure. 7. (a) Predicted moment-curvature curve for selected stents. (b) Predicted stent curvature
474 when the η_ε value first reaches a value of 1.0 in an element for all stents and materials.

475 Figure. 8. (a) Prediction of the resulting reaction force for a given longitudinal compression for
476 selected stents. (b) The force required for a 10% stent longitudinal compression for all materials
477 and stents.

478

Graphical Abstract

Click here to download high resolution image

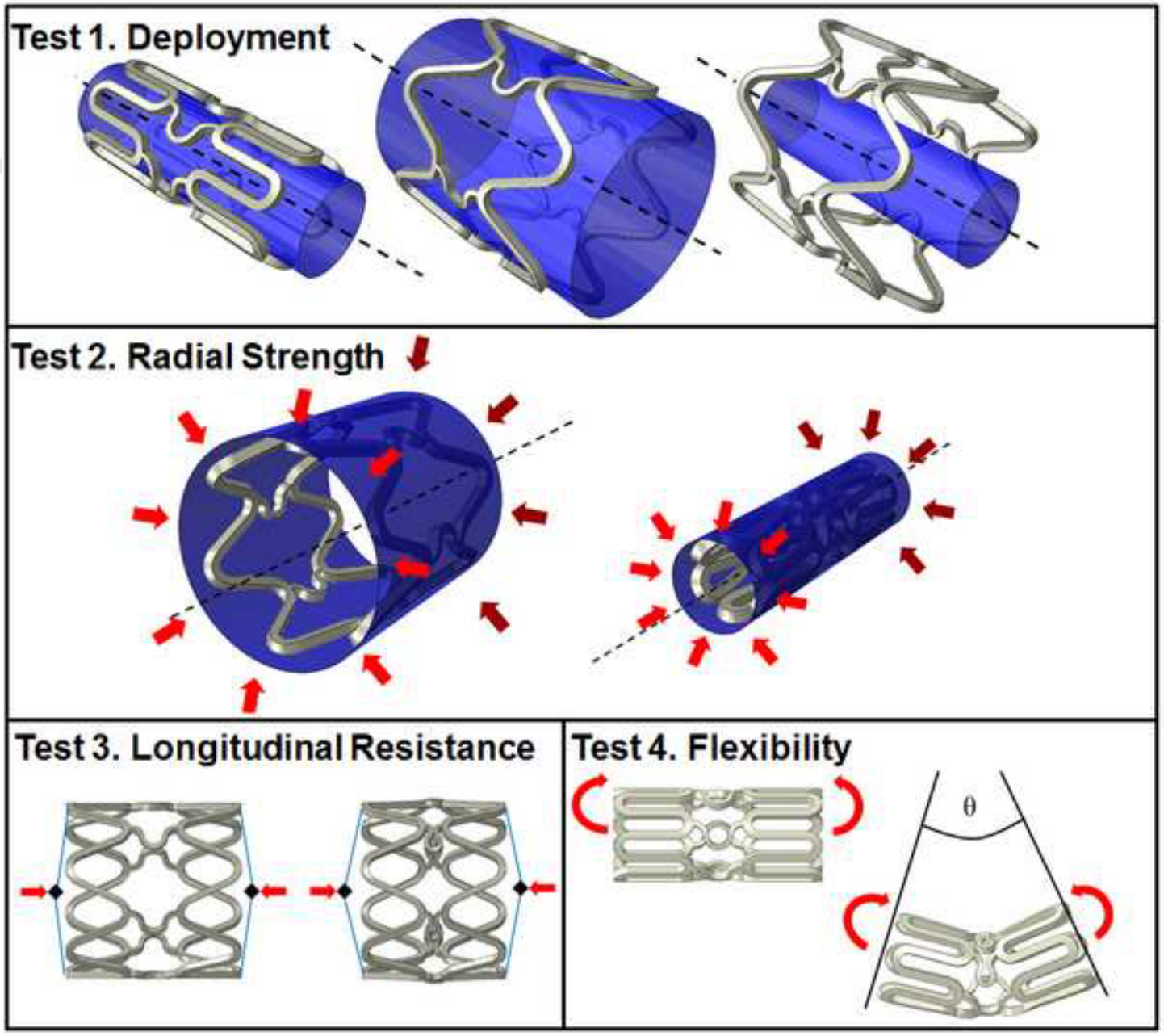

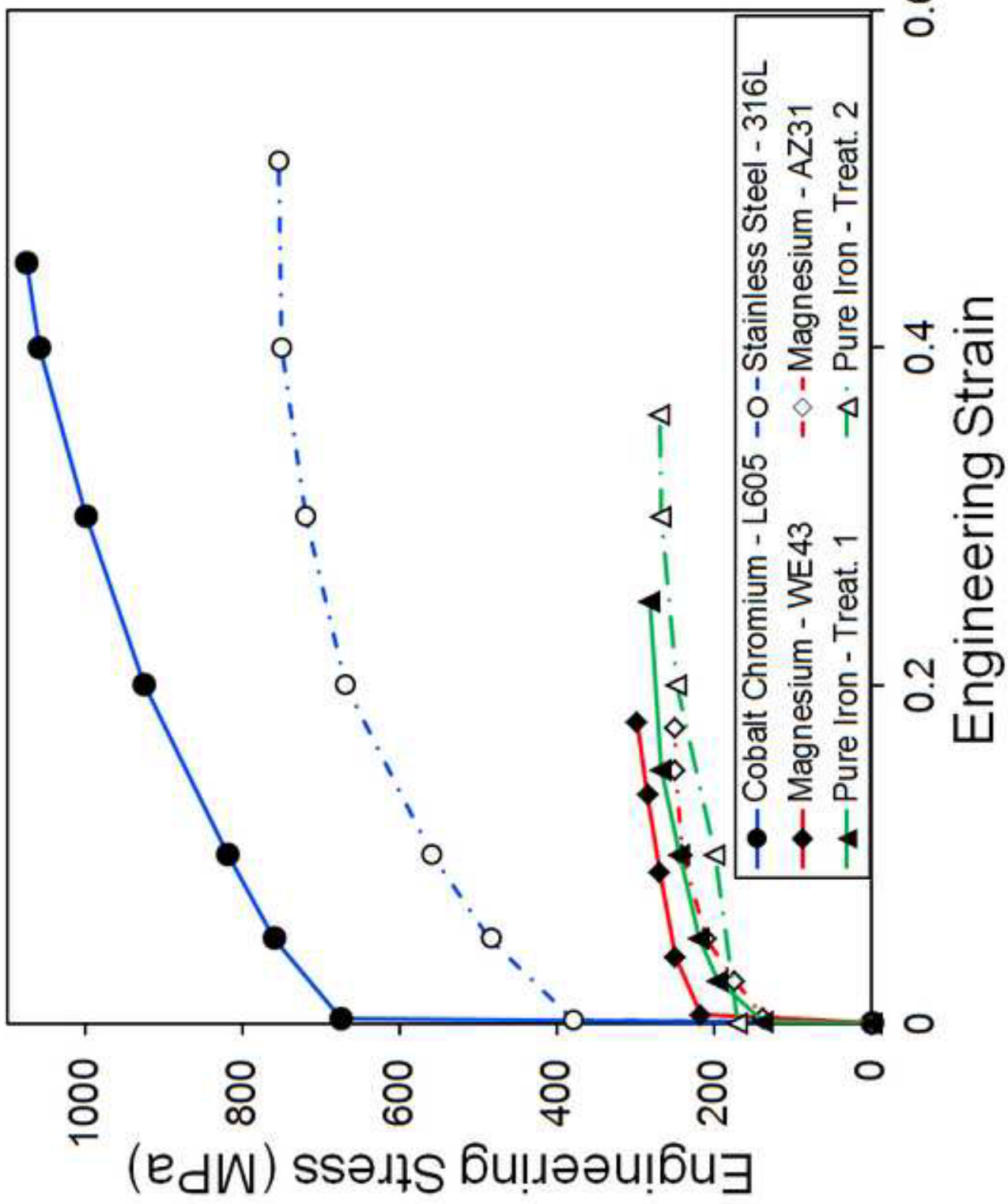

Figure 1
Click here to download high resolution image

Figure 2
Click here to download high resolution image

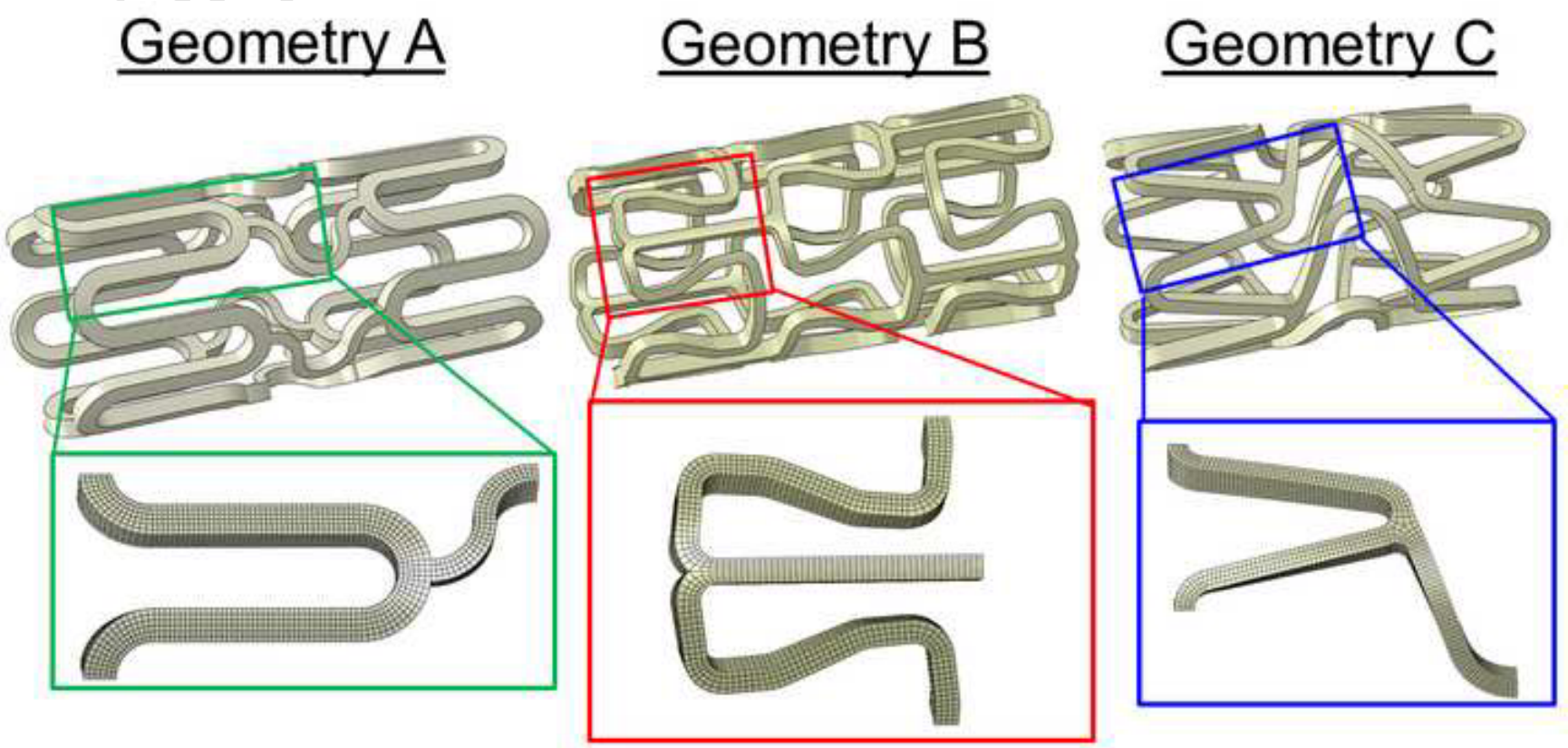

Figure 3
Click here to download high resolution image

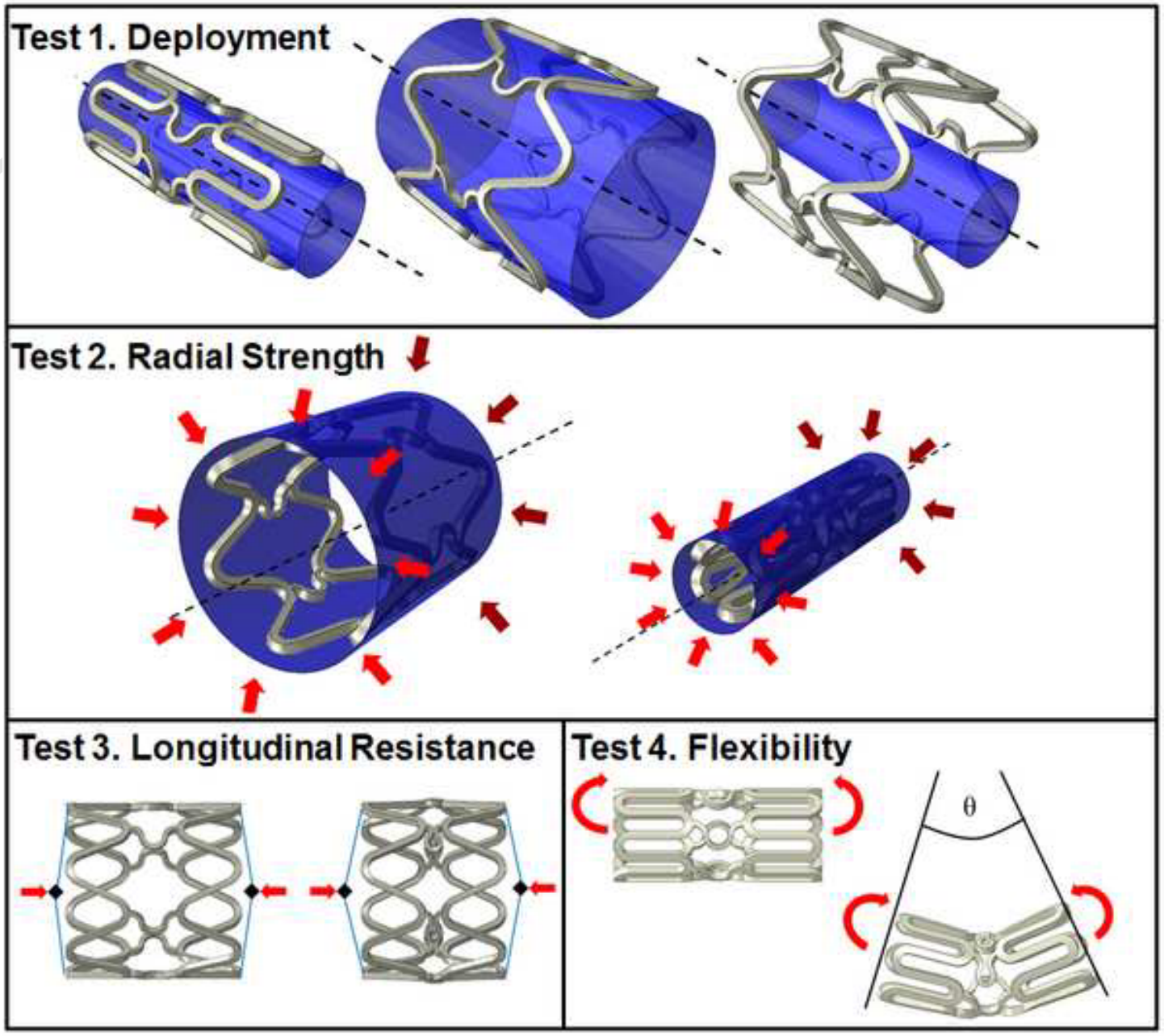

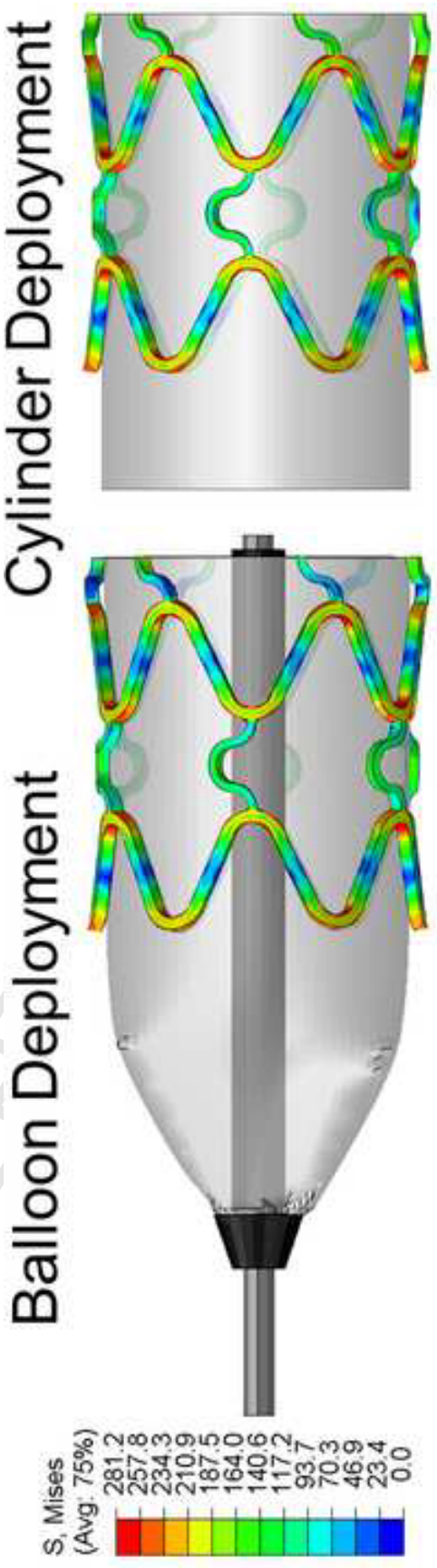

Figure 4
Click here to download high resolution image

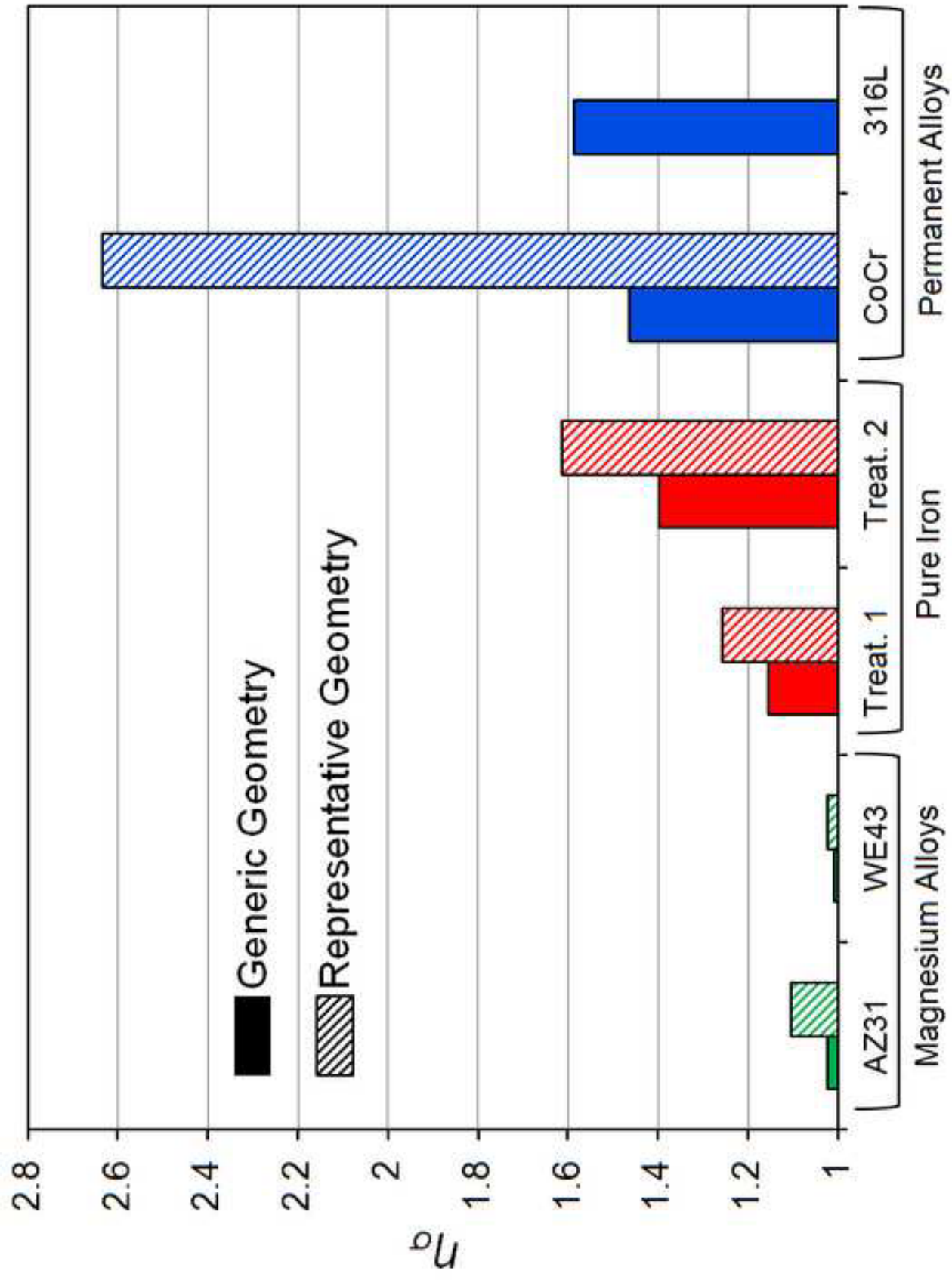

Figure 5a
Click here to download high resolution image

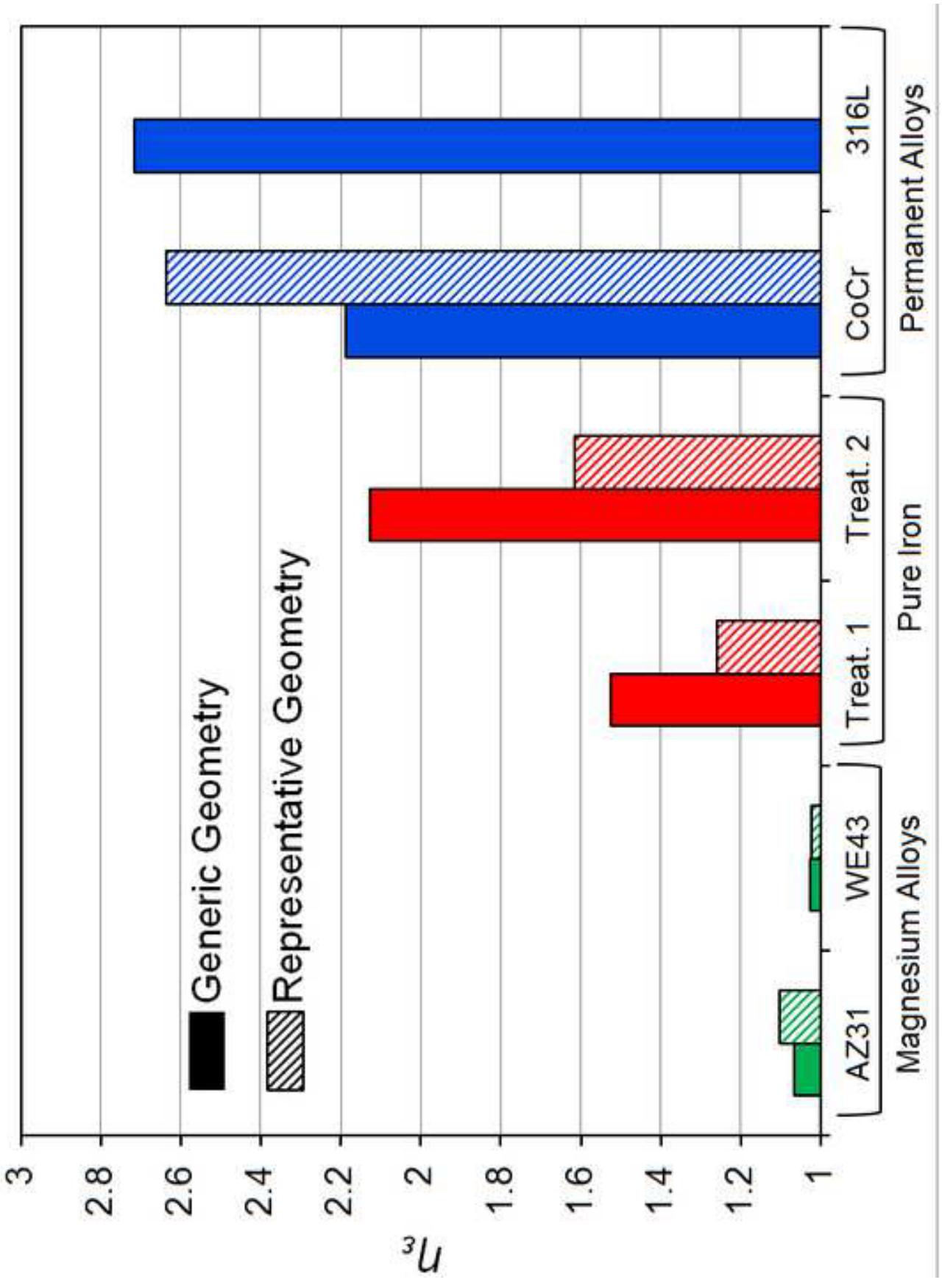

Figure 5b
Click here to download high resolution image

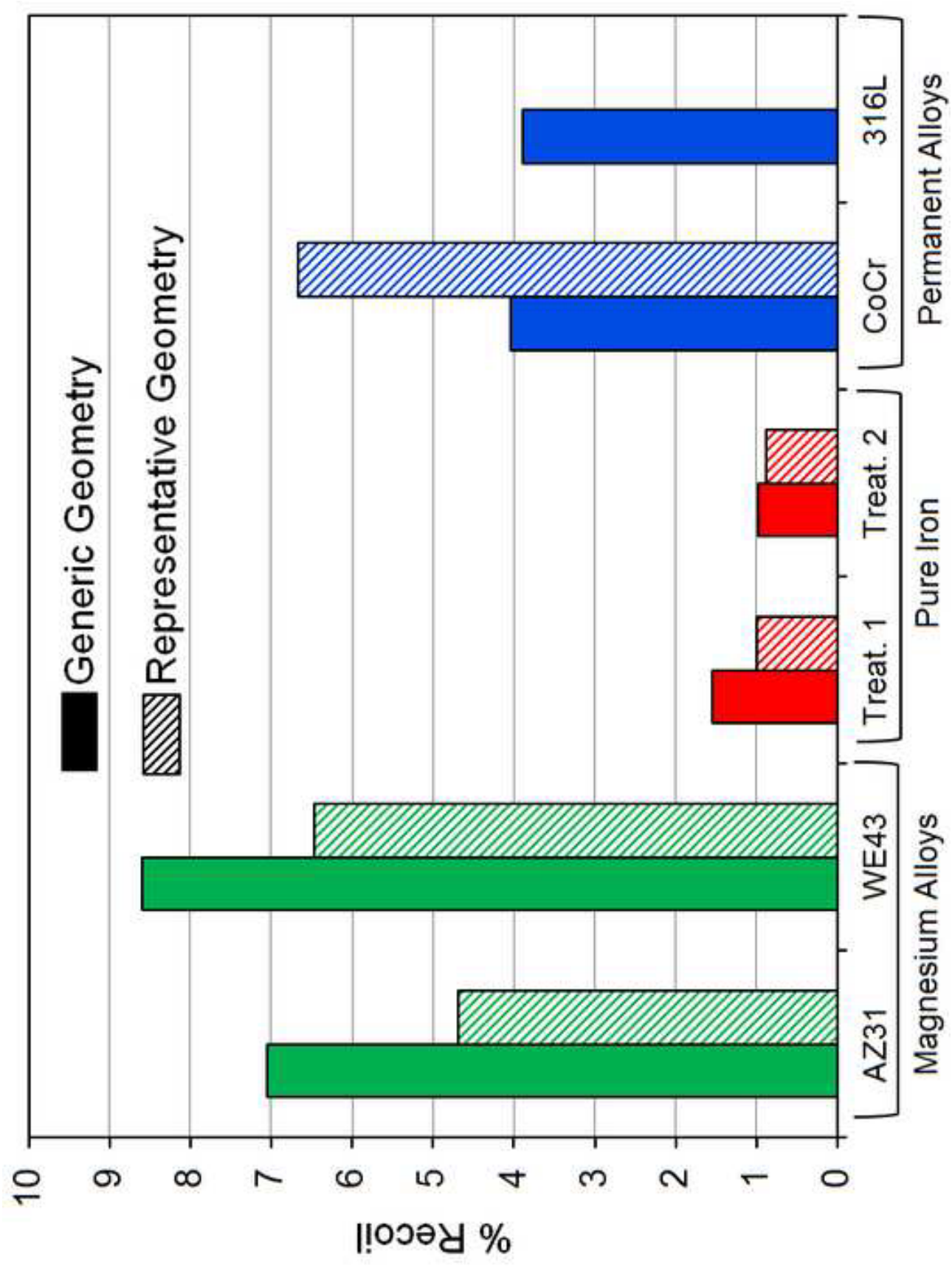

Figure 5c
Click here to download high resolution image

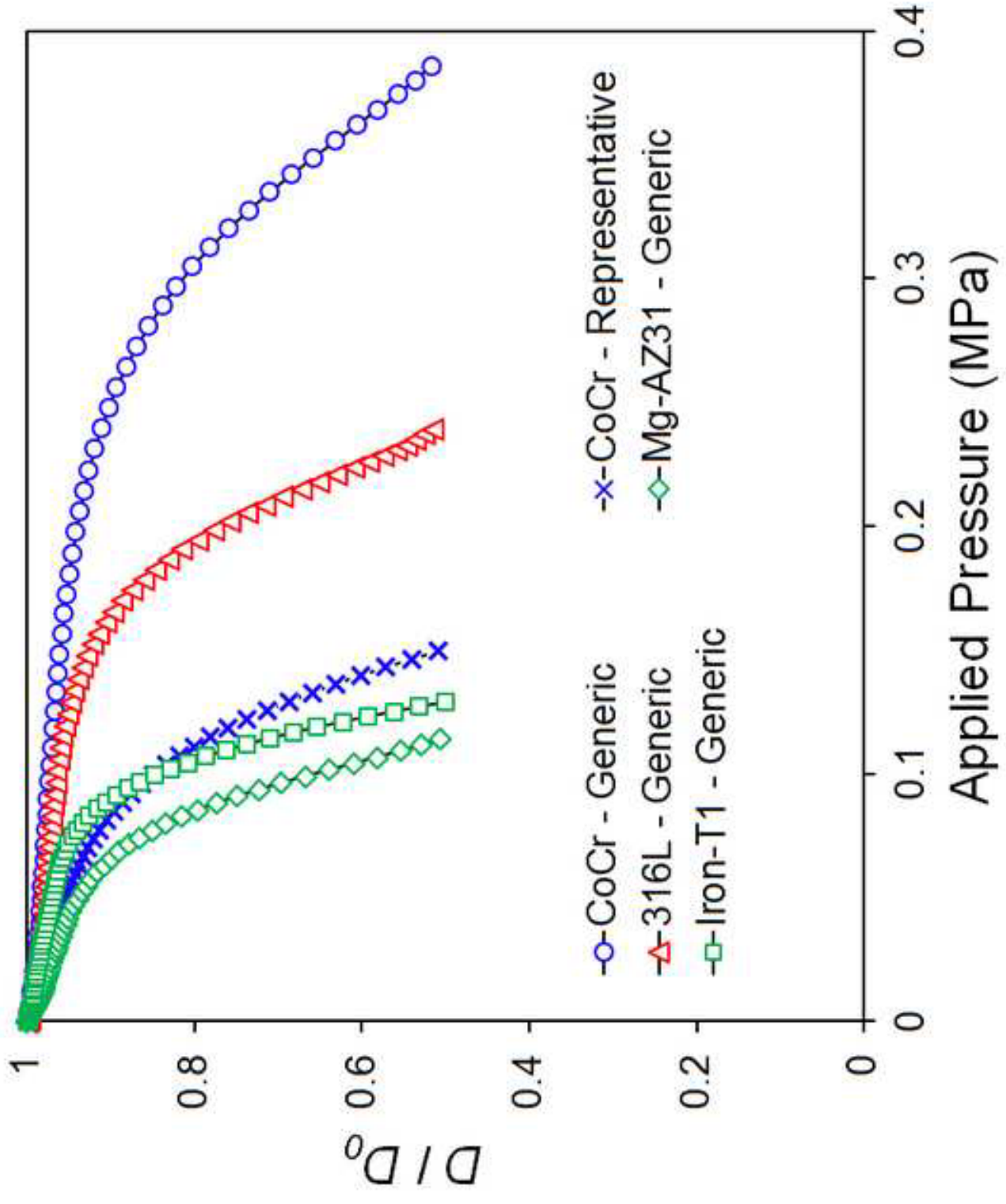

Figure 6a
Click here to download high resolution image

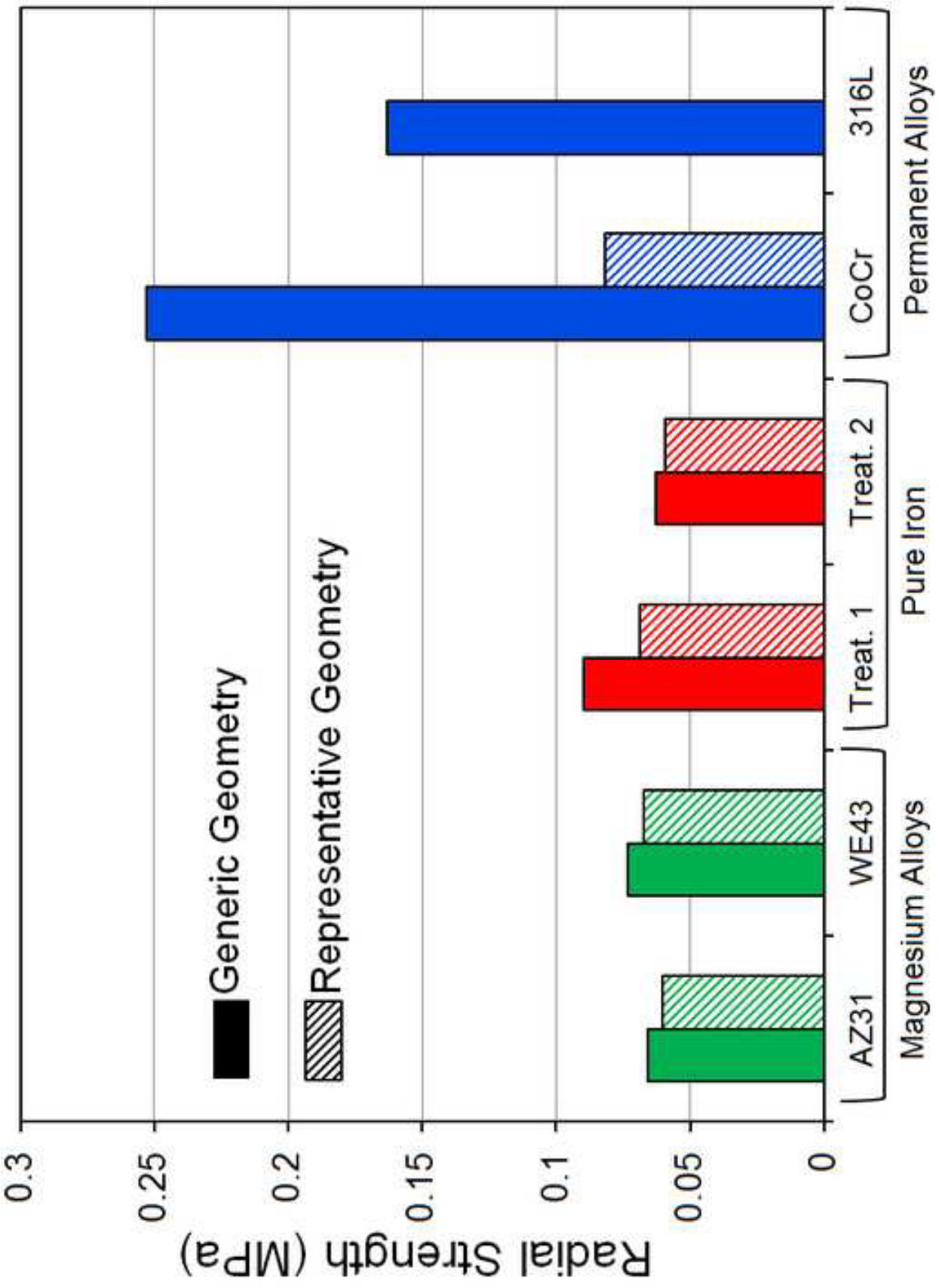

Figure 6b
Click here to download high resolution image

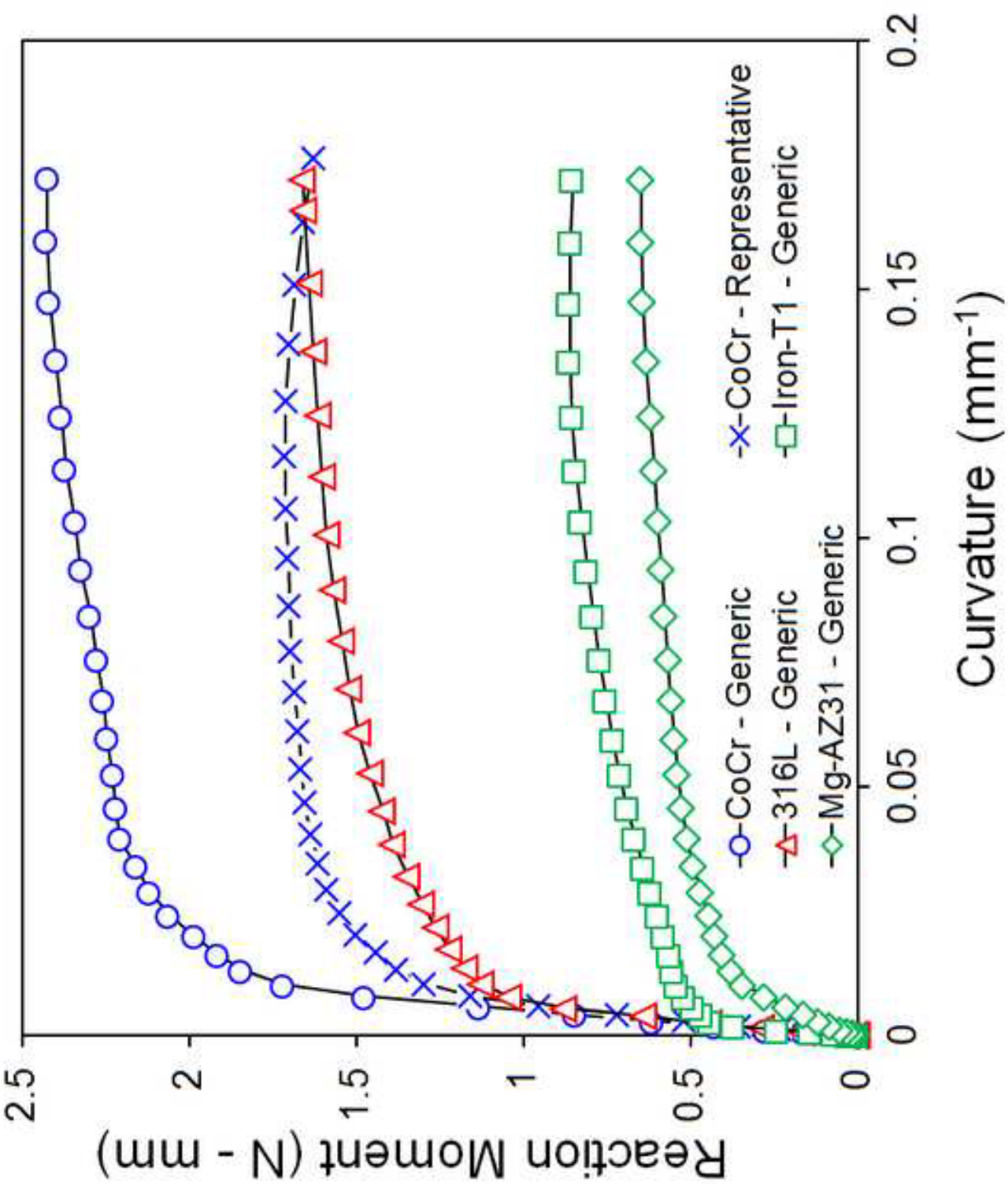

Figure 7a
Click here to download high resolution image

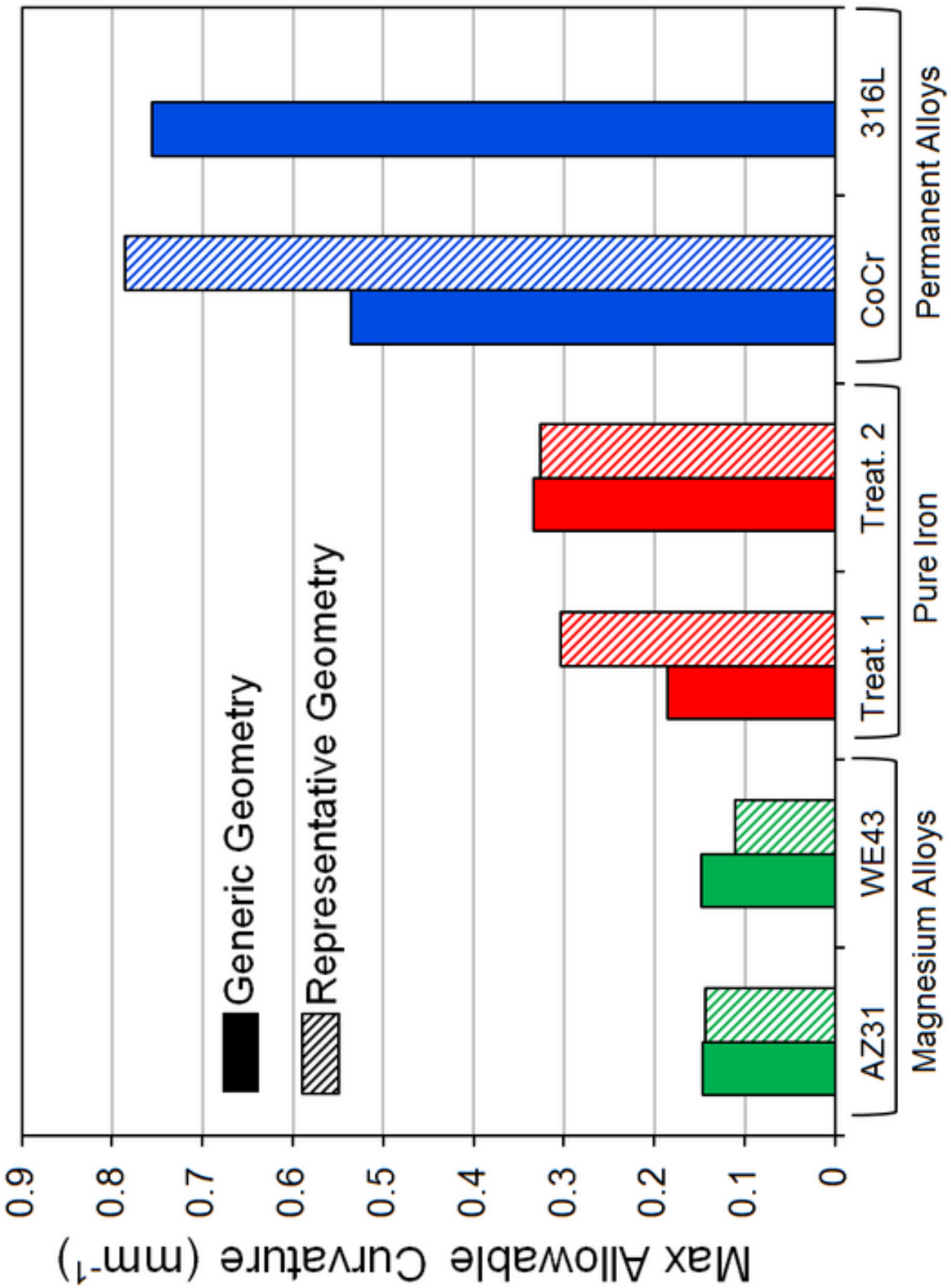

Figure 7b
Click here to download high resolution image

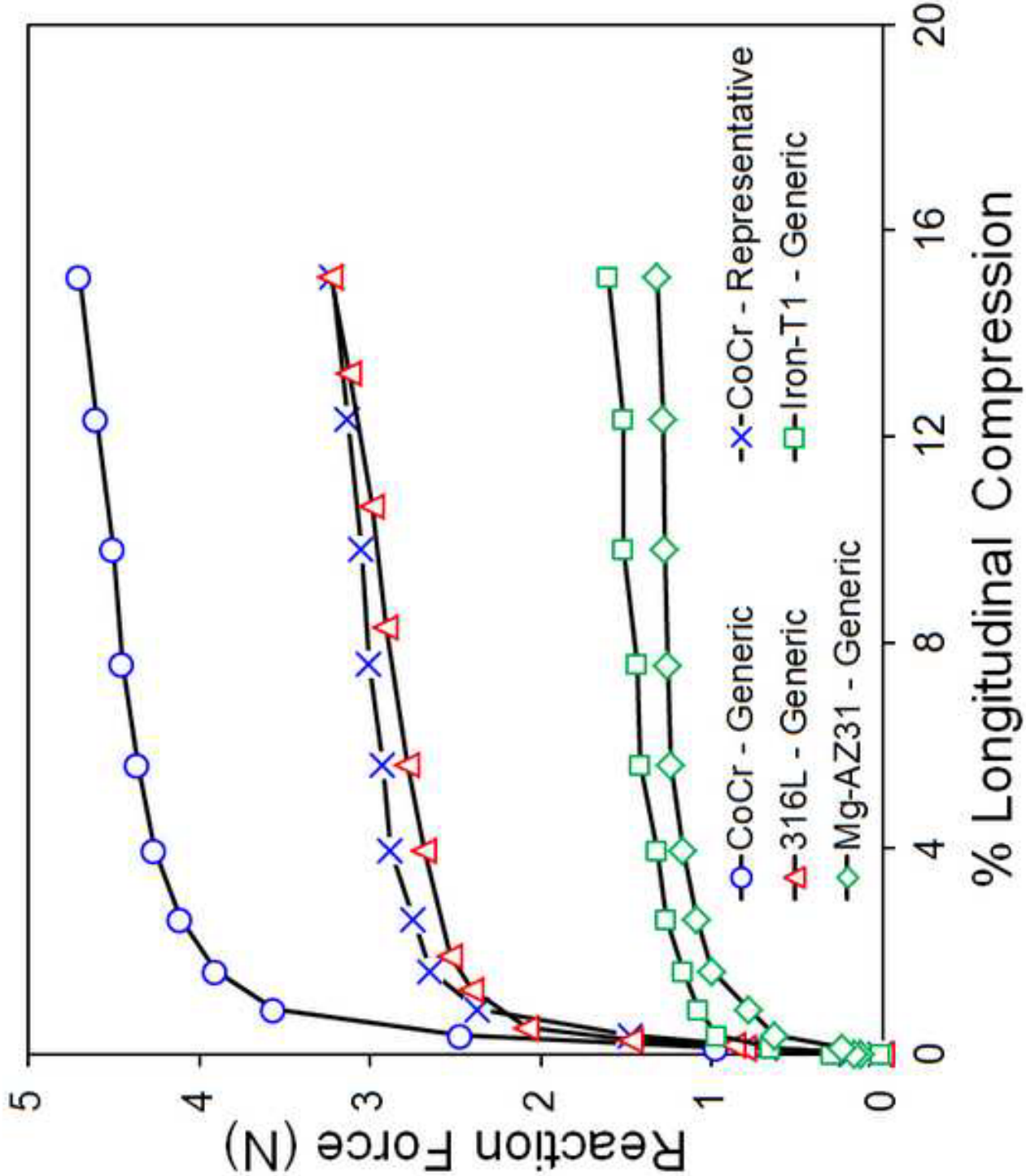

Figure 8a
Click here to download high resolution image

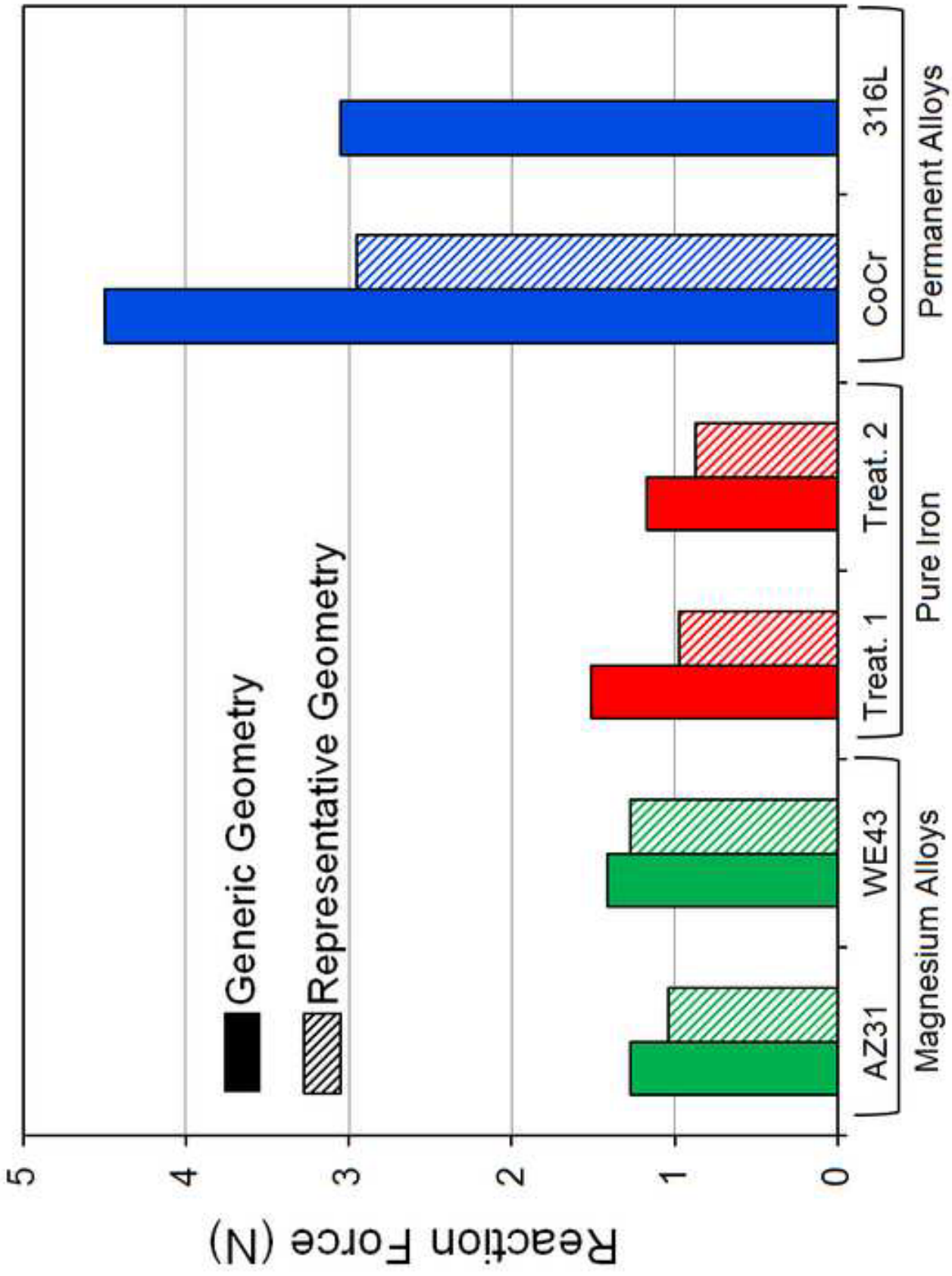

Figure 8b
Click here to download high resolution image

Comparing coronary stent material performance on a common geometric platform through simulated bench-testing.

J.A. Grogan, S.B. Leen, P.E. McHugh

Biomechanics Research Centre (BMEC), Mechanical and Biomedical Engineering, College of Engineering and Informatics, National University of Ireland, Galway, Ireland.

Highlights

- Performance of a range of metals compared on a common stent platform.
- Higher risk of fracture predicted in Mg stents relative to permanent and Fe stents.
- Similar scaffolding for AMS and permanent stents possible through stent design.
- Improvements in Mg alloy ductility important for Mg stents.
- Improvements in Fe alloy strength important for Fe stents.